

# Synthesis, crystal structure, optical, and electronic study of the new ternary thorium selenide $\text{Ba}_3\text{ThSe}_3(\text{Se}_2)_2$

Jai Prakash<sup>a</sup>, Adel Mesbah<sup>a,b</sup>, Jessica Beard<sup>a</sup>, Sébastien Lebègue<sup>c</sup>, Christos D. Malliakas<sup>a</sup>, and James A. Ibers<sup>a,\*</sup>

<sup>a</sup>*Department of Chemistry, Northwestern University, Evanston, IL 60208-3113, USA*

<sup>b</sup>*ICSM, UMR 5257 CEA / CNRS / UM2 / ENSCM, Site de Marcoule - Bât. 426, BP 17171, 30207 Bagnols-sur-Cèze cedex, France*

<sup>c</sup>*Laboratoire de Cristallographie, Résonance Magnétique et Modélisations (CRM2, UMR CNRS 7036), Institut Jean Barriol, Université de Lorraine, BP 239, Boulevard des Aiguillettes, 54506 Vandoeuvre-lès-Nancy, France*

*Keywords:* barium thorium selenide; crystal structure; optical study; band gap; DFT

## Abstract

The compound  $\text{Ba}_3\text{ThSe}_3(\text{Se}_2)_2$  has been synthesized by solid-state methods at 1173 K. Its crystal structure features one dimensional chains of  $[\text{Th}(\text{Se})_3(\text{Se}_2)_2]^{6-}$  separated by  $\text{Ba}^{2+}$  cations. Each Th atom in these chains is coordinated to two Se–Se single-bonded pairs and four Se atoms to give rise to a pseudooctahedral geometry around Th. The Th–Se distances are consistent with  $\text{Th}^{4+}$  and hence charge balance of  $\text{Ba}_3\text{ThSe}_3(\text{Se}_2)_2$  is achieved as  $3 \times \text{Ba}^{2+}$ ,  $1 \times \text{Th}^{4+}$ ,  $3 \times \text{Se}^{2-}$ , and  $2 \times \text{Se}_2^{2-}$ . From optical measurements the band gap of  $\text{Ba}_3\text{ThSe}_3(\text{Se}_2)_2$  is 1.96(2) eV. DFT calculations indicate that the compound is a semiconductor.

## 1. Introduction

Solid-state actinide chalcogenides offer diverse crystal chemistry, different stoichiometries, and a wide range of physical properties, including optical [1-3], magnetic [1-3], and transport [4,5]. These result from the presence of f-electrons and ability of the lighter actinides (An) to show variable oxidation states, and the tendency of the heavier chalcogens (Q) to show various Q–Q interactions. The crystal chemistry and properties of Th chalcogenides are

---

\*Corresponding author.

*E-mail address:* [ibers@chem.northwestern.edu](mailto:ibers@chem.northwestern.edu) (J.A.Ibers)

less known than those of U chalcogenides. Examples of binary thorium chalcogenides include ThS<sub>2</sub> [6], Th<sub>2</sub>S<sub>3</sub> [7],  $\alpha$ -ThTe<sub>3</sub> [8], Th<sub>2</sub>Q<sub>5</sub> (Q = S [9] and Se [10]), and Th<sub>7</sub>Q<sub>12</sub> (Q = S [11] and Te [12]), although the latter two are almost certainly the ternary Th<sub>7</sub>O<sub>2</sub>Q<sub>12</sub> [13]. The crystal structures of these binary compounds range from simple layered structures as in  $\alpha$ -ThTe<sub>3</sub> to complex modulated structures as in Th<sub>2</sub>Se<sub>5</sub> [10].

Ternary thorium chalcogenides involving an electropositive alkali metal (A) or alkaline-earth metal or a transition metal often show new structure types with varied physical properties. Examples of ternary thorium chalcogenides are ATh<sub>2</sub>Q<sub>6</sub> (A = K, Rb, Cs, Cu; Q = Se, Te) [14-18], Ba<sub>2</sub>ThS<sub>6</sub> [19], SrTh<sub>2</sub>Se<sub>5</sub> [18], BaTh<sub>2</sub>S<sub>5</sub> [20], MnThSe<sub>3</sub> [21], and Th<sub>0.81</sub>Mo<sub>6</sub>S<sub>8</sub> [22].

The few known quaternary thorium chalcogenides include ACuThQ<sub>3</sub> (A = K, Cs, Tl; Q = S, Se) [23-26], Ba<sub>2</sub>Cu<sub>2</sub>ThS<sub>5</sub> [27], Ba<sub>2</sub>Cu<sub>2</sub>ThSe<sub>5</sub> [28], K<sub>2</sub>Cu<sub>2</sub>ThS<sub>4</sub> [23], K<sub>3</sub>Cu<sub>3</sub>Th<sub>2</sub>S<sub>7</sub> [23], KThSb<sub>2</sub>Se<sub>6</sub> [29], and Ba<sub>2</sub>CrThTe<sub>7</sub> [30].

To extend the chemistry of thorium chalcogenides, we have carried out exploratory syntheses. Here we present the synthesis, structure, optical, and electronic properties of the new thorium chalcogenide, Ba<sub>3</sub>ThSe<sub>3</sub>(Se<sub>2</sub>)<sub>2</sub>.

## 2. Experimental

### 2.1 Syntheses

Caution! <sup>232</sup>Th is an  $\alpha$ -emitting radioisotope and as such is considered a health risk. Its use requires appropriate infrastructure and personnel trained in the handling of radioactive materials.

The starting materials Ba (Johnson Matthey, 99.5 %), Th (MP Biomedicals, 99.1 %), Sb (Alfa, 99.5 %), and Se (Cerac, 99.999 %) were used as obtained. Reactions were performed in sealed 6 mm carbon-coated fused-silica tubes. Chemical manipulations were performed inside an Ar-filled dry box. The reactants were weighed and transferred into tubes that were then evacuated to 10<sup>-4</sup> Torr, flame sealed, and placed in a computer-controlled furnace.

*Synthesis of Ba<sub>3</sub>ThSe<sub>3</sub>(Se<sub>2</sub>)<sub>2</sub>.* Dark-red block-shaped crystals of Ba<sub>3</sub>ThSe<sub>3</sub>(Se<sub>2</sub>)<sub>2</sub> were initially obtained from the reaction of Ba (35.5 mg, 0.2585 mmol), Th (10 mg, 0.0431 mmol), Sb

(10.9 mg, 0.0895 mmol), and Se (54.4 mg, 0.6890 mmol). The reaction mixture was heated to 1033 K in 36 h and held constant at this temperature for 15 h. The temperature of the furnace was then raised to 1173 K at 1.5 K/h, and the reaction mixture was annealed for 96 h followed by slow cooling to 573 K at 2 K/h and then to 298 K at 11 K/h. Semi-quantitative EDX analysis of the products of the reaction were obtained with the use of a Hitachi S-3400 SEM microscope. The reaction product contained dark-red crystals of  $\text{Ba}_3\text{ThSe}_3(\text{Se}_2)_2$  (Ba:Th:Se $\approx$ 3:1:7), black columnar crystals of  $\text{Sb}_2\text{Se}_3$  [31] (Sb:Se $\approx$ 2:3), red crystals of BaSe, copper-colored crystals of  $\text{Th}_2\text{Se}_5$  [10] (Th:Se $\approx$ 2:5), and plate-shaped red crystals of ThOSe [32]. Crystals of  $\text{Ba}_3\text{ThSe}_3(\text{Se}_2)_2$  were subsequently obtained from the stoichiometric reaction of the elements using the same heating conditions. The crystals of  $\text{Ba}_3\text{ThSe}_3(\text{Se}_2)_2$  stored in paratone oil were stable for months. However, crystals stored under ambient condition decomposed in a few weeks.

## 2.2 Crystal structure determination

The crystal structure of  $\text{Ba}_3\text{ThSe}_3(\text{Se}_2)_2$  was determined from single-crystal X-ray diffraction data collected with the use of graphite-monochromatized  $\text{MoK}\alpha$  radiation ( $\lambda = 0.71073 \text{ \AA}$ ) at 100(2) K on a Bruker APEX2 diffractometer [33]. The algorithm COSMO implemented in the program APEX2 was used to establish the data collection strategy with a series of  $0.3^\circ$  scans in  $\omega$  and  $\varphi$ . The exposure time was 10 s/frame and the crystal-to-detector distance was 60 mm. The collection of intensity data as well as cell refinement and data reduction were carried out with the use of the program APEX2 [33]. Face-indexed absorption, incident beam, and decay corrections were performed with the use of the program SADABS [34]. Precession images of the data set provided no evidence for a super cell or for modulation. The structure was solved and refined in a straightforward manner with the use of the SHELX-14 algorithms of the SHELXL program package [34,35]. The program STRUCTURE TIDY [36] in PLATON [37] was used to standardize the atomic positions. Further details are given in Table 1 and in the Supporting information.

### 2.3 Optical study

Single-crystal absorption spectra were obtained at 298 K on a Hitachi U-6000 Microscopic FT spectrophotometer mounted on an Olympus BH2-UMA microscope. A single crystal of  $\text{Ba}_3\text{ThSe}_3(\text{Se}_2)_2$  was placed on a glass slide and positioned over the light source where the transmitted light was recorded from above. The background signal of the glass slide was subtracted from the collected intensity.

### 2.4. Theoretical calculations

Density functional theory [38,39] and the Heyd-Scuseria-Ernzerhof (HSE) [40-42] exchange-correlation functional were used for the calculations. The Vienna ab Initio Simulation Package [43,44] implementing the projector augmented wave method [45] was employed. The atomic positions and cell parameters were taken from the crystal-structure results. The Brillouin zone was sampled with a  $4 \times 8 \times 6$  mesh, and the default cut-off for the plane-wave part of the wave function was used.

## 3. Results

### 3.1 Synthesis and structure of $\text{Ba}_3\text{ThSe}_3(\text{Se}_2)_2$

Single crystals of  $\text{Ba}_3\text{ThSe}_3(\text{Se}_2)_2$  were initially obtained at 1173 K in about 10 wt% yield in an attempt to discover a new quaternary compound in the Ba/Th/Sb/Se system. Synthesis of dark-red crystals of  $\text{Ba}_3\text{ThSe}_3(\text{Se}_2)_2$  were reproduced by the stoichiometric reaction of the elements using the same heating conditions. However, the yield was still low (about 20 wt%) and the major products were  $\text{Th}_2\text{Se}_5$  [10] and BaSe. Further attempts to improve the yield of  $\text{Ba}_3\text{ThSe}_3(\text{Se}_2)_2$  by varying the heating conditions were unsuccessful.

A view of the crystal structure of  $\text{Ba}_3\text{ThSe}_3(\text{Se}_2)_2$  is shown in Fig. 1. The compound crystallizes in a new structure type with two formula units in the noncentrosymmetric space group  $C_{2v}^{20} - \text{Imm}2$  of the orthorhombic crystal system with cell constants  $a = 12.4213(1)$ ,  $b =$

5.7911(1), and  $c = 9.5039(1)$  Å. Metrical data for  $\text{Ba}_3\text{ThSe}_3(\text{Se}_2)_2$  are presented in Table 2 and in the Supporting information. The asymmetric unit of the structure comprises one Th atom (site symmetry  $mm2$ ), two Ba atoms (Ba1 ( $.m.$ ), Ba2 ( $mm2$ )), and four Se atoms (Se1 ( $.m.$ ), Se2 ( $.m.$ ), Se3 ( $m.$ ), and Se4 ( $mm2$ )). The structure consists of one-dimensional chains of  $^1 \infty[\text{Th}(\text{Se})_3(\text{Se}_2)_2]^{6-}$  separated by  $\text{Ba}^{2+}$  cations (Fig. 1). These one-dimensional chains run along the  $b$ -axis. Each Th atom in these chains is coordinated to two Se–Se pairs (Se1–Se1 and Se3–Se3), two Se2 atoms, and two Se4 atoms to give rise to a pseudooctahedral geometry around Th (Fig. 2). The geometry of the Th polyhedron in the structure of  $\text{Ba}_3\text{ThSe}_3(\text{Se}_2)_2$  is similar to the An polyhedra in the structures of  $\text{Ba}_2\text{AnS}_6$  (An = Th and U) [19] but the connectivity of these polyhedra is very different (Fig. 4). Th atoms in  $\text{Ba}_3\text{ThSe}_3(\text{Se}_2)_2$  are connected to each other through Se4 atoms in the  $b$ -direction forming a one-dimensional chain whereas in the structure of  $\text{Ba}_2\text{AnS}_6$ , the  $\text{AnS}_8$  polyhedra share two corners along the  $a$  and  $b$  axes to result in a two-dimensional structure.

The Se–Se distances of 2.3737(9) and 2.3771(9) Å in this structure are typical for Se–Se single bonds of  $\text{Se}_2^{2-}$  units, for example in  $\text{KAuSe}_5$  (2.362(1) to 2.343(1) Å) [46],  $\text{Ba}_8\text{PdU}_2\text{Se}_{12}(\text{Se}_2)_2$  (2.392(1) and 2.407(1) Å) [47],  $\text{Cs}_4\text{Ge}_2\text{Se}_8$  (2.350 Å) [48],  $\text{CsAuSe}_3$  (2.384 Å) [49],  $\text{KU}_2\text{SbSe}_8$  (2.356(5) to 2.375(4) Å) [50],  $\text{USe}_3$  (2.361 Å) [51], and  $\text{RbPdCu}(\text{Se}_2)(\text{Se}_3)$  (2.338(2) Å) [52]. The Th–Se distances of 2.9299(4)–3.0496(5) Å are comparable with  $\text{Th}^{4+}$ –Se distances in related compounds (Table 3). Hence, charge balance of  $\text{Ba}_3\text{ThSe}_3(\text{Se}_2)_2$  is achieved as  $3 \times \text{Ba}^{2+}$ ,  $1 \times \text{Th}^{4+}$ ,  $3 \times \text{Se}^{2-}$ , and  $2 \times \text{Se}_2^{2-}$ .

The Ba1 atoms in  $\text{Ba}_3\text{ThSe}_3(\text{Se}_2)_2$  are surrounded by seven Se atoms in a distorted monocapped trigonal-prismatic fashion whereas the Ba2 atoms are surrounded by nine Se atoms in a tricapped trigonal-prismatic fashion (Fig. 3). The Ba–Se distances (3.2599(5) to 3.5292(5) Å) in the  $\text{BaSe}_7$  and  $\text{BaSe}_9$  polyhedra are normal. The  $\text{BaSe}_9$  polyhedron in this structure is very similar to that in the structure of  $\text{BaThTe}_4$  [53].

### 3.2 Optical study

The optical absorption spectrum collected at 298 K on a thin single crystal of  $\text{Ba}_3\text{ThSe}_3(\text{Se}_2)_2$  (Fig. 5) shows a band gap transition at 1.96(2) eV, consistent with its dark red color. Analysis of the square and square root of the absorptivity ( $\alpha$ ) as a function of energy (Fig.6) gives a direct band gap of 1.99(2) eV and an indirect band gap of 1.95(2) eV.

### 3.3 Theoretical calculations

The total and partial density of states (DOS) of  $\text{Ba}_3\text{ThSe}_3(\text{Se}_2)_2$  are presented in Fig. 7. From the total density of states (upper plot of Fig. 7),  $\text{Ba}_3\text{ThSe}_3(\text{Se}_2)_2$  is found to be a semiconductor with a band gap of 1.5 eV, compared with the experimental value of 1.96 eV. As expected, no sign of spin polarization is detected, as seen by the totally symmetric DOS for the spin up and the spin down. Also, the top of the valence states corresponds mainly to Se-p states together with Th-f states whereas the bottom of the conduction states corresponds mainly to Se-p states mixed with Ba-d states.

## 4. Conclusions

The compound  $\text{Ba}_3\text{ThSe}_3(\text{Se}_2)_2$  has been synthesized in approximately 20 wt% yield by solid-state methods at 1173 K. The dark-red compound crystallizes in a new structure type with two formula units in the noncentrosymmetric space group  $C_{2v}^{20}-Imm2$  of the orthorhombic crystal system with cell constants  $a = 12.4213(1)$ ,  $b = 5.7911(1)$ , and  $c = 9.5039(1)$  Å. Its crystal structure features one dimensional chains of  $\frac{1}{\infty}[\text{Th}(\text{Se})_3(\text{Se}_2)_2^{6-}]$  separated by  $\text{Ba}^{2+}$  cations. Each Th atom in these chains is coordinated to two Se–Se single-bonded pairs and four Se atoms to give rise to a pseudooctahedral geometry around Th. The Th–Se distances are consistent with those in a number of  $\text{Th}^{4+}$  compounds and hence charge balance of  $\text{Ba}_3\text{ThSe}_3(\text{Se}_2)_2$  is achieved as  $3 \times \text{Ba}^{2+}$ ,  $1 \times \text{Th}^{4+}$ ,  $3 \times \text{Se}^{2-}$ , and  $2 \times \text{Se}_2^{2-}$ . Analysis of the square and square root of the absorptivity ( $\alpha$ ) as a function of energy gives a direct band gap of 1.99(2) eV and an indirect band gap of 1.95(2) eV. DFT calculations indicate that the compound is a semiconductor and predict a band gap of 1.5 eV. The top of the valence states corresponds mainly to Se-p states

together with Th-f states whereas the bottom of the conduction states corresponds mainly to Se-p states mixed with Ba-d states.

## Acknowledgments

Use was made of the IMSERC X-ray Facility at Northwestern University, supported by the International Institute of Nanotechnology (IIN). S. L. acknowledges HPC resources from GENCI-CCRT/CINES (Grant x2015-085106). Parts of the calculations were performed in the Computing Centre of the Slovak Academy of Sciences using the supercomputing infrastructure acquired in project ITMS26230120002 and 26210120002 (Slovak Infrastructure for High-performance Computing) supported by the Research and Development Operational Programme funded by the ERDF. C.D.M. was supported by the U.S. Department of Energy, Office of Basic Energy Sciences, under Contract DE-AC02-06CH11357.

## Appendix A. Supporting information

Crystallographic data in cif format for  $\text{Ba}_3\text{ThSe}_3(\text{Se}_2)_2$  have been deposited with FIZ Karlsruhe as CSD number 429804. These data may be obtained free of charge by contacting FIZ Karlsruhe at +497247808666 (fax) or [crysdata@fiz-karlsruhe.de](mailto:crysdata@fiz-karlsruhe.de) (email).

## References

- [1] A.J. Freeman, J.B. Darby Jr., *The Actinides: Electronic Structure and Related Properties*, vol. 1, 2, Academic Press, New York, 1974.
- [2] D.E. Bugaris, J.A. Ibers, *Dalton Trans.* 39 (2010) 5949-5964.
- [3] E. Manos, M.G. Kanatzidis, J.A. Ibers, *Actinide Chalcogenide Compounds*, in: L.R. Morss, N.M. Edelstein, J. Fuger (Eds.), *The Chemistry of the Actinide and Transactinide Elements*, 4th ed., Vol. 6, Springer, Dordrecht, The Netherlands, 2010, p. 4005-4078.
- [4] D. Damien, C.H. de Novion, J. Gal, *Solid State Commun.* 38 (1981) 437-440.
- [5] C.H. de Novion, D. Damien, H. Hubert, *J. Solid State Chem.* 39 (1981) 360-367.
- [6] G. Amoretti, G. Calestani, D.C. Giori, *Z. Naturforsch. A: Phys. Phys. Chem. Kosmophys.* 39 (1984) 778-782.
- [7] W.H. Zachariasen, *Acta Cryst.* 2 (1949) 291-296.
- [8] J. Prakash, J.A. Ibers, *Z. Anorg. Allg. Chem.* 640 (2014) 1943-1945.
- [9] H. Noël, M. Potel, *Acta Crystallogr. Sect. B: Struct. Crystallogr. Cryst. Chem.* 38 (1982) 2444-2445.
- [10] B.J. Bellott, C.D. Malliakas, L.A. Koscielski, M.G. Kanatzidis, J.A. Ibers, *Inorg. Chem.* 52 (2013) 944-949.
- [11] W.H. Zachariasen, *Acta Cryst.* 2 (1949) 288-291.

- [12] O. Tougait, M. Potel, H. Noël, *Inorg. Chem.* 37 (1998) 5088-5091.
- [13] M.D. Ward, J.A. Ibers, *Z. Anorg. Allg. Chem.* 640 (2014) 1585-1588.
- [14] E.J. Wu, M.A. Pell, J.A. Ibers, *J. Alloys Compd.* 255 (1997) 106-109.
- [15] K.-S. Choi, R. Patschke, S.J.L. Billinge, M.J. Waner, M. Dantus, M.G. Kanatzidis, *J. Am. Chem. Soc.* 120 (1998) 10706-10714.
- [16] J.A. Cody, J.A. Ibers, *Inorg. Chem.* 35 (1996) 3836-3838.
- [17] D.E. Bugaris, D.M. Wells, J. Yao, S. Skanthakumar, R.G. Haire, L. Soderholm, J.A. Ibers, *Inorg. Chem.* 49 (2010) 8381-8388.
- [18] A.A. Narducci, J.A. Ibers, *Inorg. Chem.* 37 (1998) 3798-3801.
- [19] A. Mesbah, E. Ringe, S. Lebègue, R.P. Van Duyne, J.A. Ibers, *Inorg. Chem.* 51 (2012) 13390-13395.
- [20] J. Prakash, M.S. Tarasenko, A. Mesbah, S. Lebègue, C.D. Malliakas, J.A. Ibers, *Inorg. Chem.* 53 (2014) 11626-11632.
- [21] I. Ijjaali, K. Mitchell, F.Q. Huang, J.A. Ibers, *J. Solid State Chem.* 177 (2004) 257-261.
- [22] A. Daoudi, M. Potel, H. Noël, *J. Alloys Compd.* 232 (1996) 180-185.
- [23] H.D. Selby, B.C. Chan, R.F. Hess, K.D. Abney, P.K. Dorhout, *Inorg. Chem.* 44 (2005) 6463-6469.

- [24] A.A. Narducci, J.A. Ibers, *Inorg. Chem.* 39 (2000) 688-691.
- [25] L.A. Koscielski, J.A. Ibers, *Z. Anorg. Allg. Chem.* 638 (2012) 2585-2593.
- [26] L.A. Koscielski, J.A. Ibers, *Acta Cryst. Sect. E: Struct. Rep. Online* 52 (2012) i52-i53.
- [27] A. Mesbah, Lebegue.S, J.M. Klingsporn, W. Stojko, R.P. Van Duyne, J.A. Ibers, *J. Solid State Chem.* 200 (2013) 349-353.
- [28] A. Mesbah, J. Prakash, J. C. Beard, S. Lebègue, C. D. Malliakas, J. A. Ibers, Unpublished.
- [29] K.-S. Choi, L. Iordanidis, K. Chondroudís, M.G. Kanatzidis, *Inorg. Chem.* 36 (1997) 3804-3805.
- [30] J. Prakash, A. Mesbah, J. Beard, S. Lebègue, C.D. Malliakas, J.A. Ibers, *Inorg. Chem.* 54 (2015) 3688-3694.
- [31] N.W. Tideswell, F.H. Kruse, J.D. McCullough, *Acta Cryst.* 10 (1957) 99-102.
- [32] L.A. Koscielski, E. Ringe, R.P. Van Duyne, D.E. Ellis, J.A. Ibers, *Inorg. Chem.* 51 (2012) 8112-8118.
- [33] Bruker APEX2 Version 2009.5-1 Data Collection and Processing Software,, Bruker Analytical X-Ray Instruments, Inc., Madison, WI, USA, 2009.
- [34] G.M. Sheldrick, SADABS, 2008. Department of Structural Chemistry, University of Göttingen, Göttingen, Germany

- [35] G.M. Sheldrick, *Acta Crystallogr. Sect. A: Found. Crystallogr.* 64 (2008) 112-122.
- [36] L.M. Gelato, E. Parthé, *J. Appl. Crystallogr.* 20 (1987) 139-143.
- [37] A.L. Spek, *PLATON, A Multipurpose Crystallographic Tool*, 2014. Utrecht University, Utrecht, The Netherlands
- [38] W. Kohn, L.J. Sham, *Phys. Rev.* 140 (1965) 1133-1138.
- [39] P. Hohenberg, W. Kohn, *Phys. Rev.* 136 (1964) 864-871.
- [40] J. Heyd, G.E. Scuseria, M. Ernzerhof, *J. Phys. Chem.* 118 (2003) 8207-8215.
- [41] A. Durif, *Acta Cryst.* 9 (1956) 533.
- [42] J. Paier, M. Marsman, K. Hummer, G. Kresse, I.C. Gerber, J.G. Angyan, *J. Chem. Phys.* 124 (2006) 154709.
- [43] G. Kresse, J. Forthmüller, *Comput. Mater. Sci.* 6 (1996) 15-50.
- [44] G. Kresse, D. Joubert, *Phys. Rev. B* 59 (1999) 1758-1775.
- [45] P.E. Blöchl, *Phys. Rev. B* 50 (1994) 17953-17979.
- [46] Y. Park, M.G. Kanatzidis, *Angew. Chem., Int. Ed. Engl.* 29 (1990) 914-915.
- [47] J. Prakash, A. Mesbah, S. Lebègue, C. D. Malliakas, J. A. Ibers, DOI: 10.1016/j.jssc.2015.06.033.
- [48] W.S. Sheldrick, B. Schaaf, *Z. Naturforsch. B: Anorg. Chem. Org. Chem.* 49 (1994) 655-

659.

- [49] Y. Park, M.G. Kanatzidis, *J. Alloys Compd.* 257 (1997) 137-145.
- [50] K.-S. Choi, M.G. Kanatzidis, *Chem. Mater.* 11 (1999) 2613-2618.
- [51] A. Ben Salem, A. Meerschaut, J. Rouxel, *C. R. Acad. Sci., Sér. 2* 299 (1984) 617-619.
- [52] X. Chen, K.J. Dilks, X. Huang, J. Li, *Inorg. Chem.* 42 (2003) 3723-3727.
- [53] J. Prakash, S. Lebègue, C.D. Malliakas, J.A. Ibers, *Inorg. Chem.* 53 (2014) 12610-12616.
- [54] L.A. Koscielski, C.D. Malliakas, A.A. Sarjeant, J.A. Ibers, *J. Solid State Chem.* 205 (2013) 35-38.
- [55] L.A. Koscielski, E.A. Pozzi, R.P. Van Duyne, J.A. Ibers, *J. Solid State Chem.* 205 (2013) 1-4.

**Table 1**Crystallographic data and structure refinement details for  $\text{Ba}_3\text{ThSe}_3(\text{Se}_2)_2$ .

$\text{Ba}_3\text{ThSe}_3(\text{Se}_2)_2$	
Space group	$C_{2v}^{20} - Imm2$
$a$ (Å)	12.4213(2)
$b$ (Å)	5.7911(1)
$c$ (Å)	9.5039(1)
$V$ (Å <sup>3</sup> )	683.65(2)
$Z$	2
$\rho$ (g cm <sup>-3</sup> )	5.814
$\mu$ (mm <sup>-1</sup> )	37.95
$R(F)^b$	0.008
$R_w(F_o^2)^c$	0.017

<sup>a</sup> $\lambda = 0.71073$  Å,  $T = 100(2)$  K.

<sup>b</sup> $R(F) = \Sigma ||F_o| - |F_c|| / \Sigma |F_o|$  for  $F_o^2 > 2\sigma(F_o^2)$ .

<sup>c</sup> $R_w(F_o^2) = \{\Sigma [w(F_o^2 - F_c^2)^2] / \Sigma wF_o^4\}^{1/2}$ . For  $F_o^2 < 0$ ,  $w^{-1} = \sigma^2(F_o^2)$ ; for  $F_o^2 \geq 0$ ,  $w^{-1} = \sigma^2(F_o^2)$ .

**Table 2**Selected interatomic lengths (Å) for Ba<sub>3</sub>ThSe<sub>3</sub>(Se<sub>2</sub>)<sub>2</sub>.

Ba <sub>3</sub> ThSe <sub>3</sub> (Se <sub>2</sub> ) <sub>2</sub>	
Th1–Se1	3.0496(5) × 2
Th1–Se2	2.9299(5) × 2
Th1–Se3	3.0119(5) × 2
Th1–Se4	2.9522(1) × 2
Ba1–Se1	3.5292(5)
Ba1–Se2	3.2599(5) 3.2744(2) × 2
Ba1–Se3	3.3270(3) × 2
Ba1–Se4	3.2743(3)
Ba2–Se1	3.3070(3) × 4
Ba2–Se2	3.3419(5) × 2
Ba2–Se3	3.3290(6) × 2
Ba2–Se4	3.3028(8)
Se1–Se1	2.3737(9)
Se3–Se3	2.3771(9)
Th1•••Th1	5.7911(1) × 2

Table 3

Th–Se and Se–Se interactions in some related compounds with 8-coordinated Th atoms<sup>a</sup>.

Compound	Structure	Th–Se (Å)	Se–Se (Å)	Th Geometry	Ref.
Ba <sub>3</sub> ThSe <sub>3</sub> (Se <sub>2</sub> ) <sub>2</sub>	1D	2.930(1)–3.050(1)	2.374(1) 2.377(1)	8, poct	this work
SrTh <sub>2</sub> Se <sub>5</sub> <sup>b</sup>	3D	2.820(2)–3.116(2)	-	8, bctp	[18]
KTh <sub>2</sub> Se <sub>6</sub>	Layered	2.962(1)–3.015(1)	2.727(1), 2.907(1)	8, bctp	[15]
CsTh <sub>2</sub> Se <sub>6</sub>	Layered	2.959(1)–3.006(1)	2.698(3), 2.924(3)	8, bctp	[17]
RbTh <sub>2</sub> Se <sub>6</sub>	Layered	2.965(1)–3.014(1)	2.728(1), 2.906(1)	8, bctp	[15]
Th <sub>2</sub> GeSe <sub>5</sub> <sup>c</sup>	3D	2.959(1)–3.017(1)	-	8, bctp	[54]
Rb <sub>2</sub> Th <sub>7</sub> Se <sub>15</sub> <sup>d</sup>	3D	2.879(1)–3.124(1)	-	8, d-sqap	[55]
ThMnSe <sub>3</sub>	3D	2.931(1)–3.161(1)	-	8, bctp	[21]

<sup>a</sup>Some distances have been rounded for comparison. All the compounds contain Th<sup>4+</sup>.<sup>b</sup>Structure also contains seven-coordinate Th atom.<sup>c</sup>Structure also contains nine-coordinate Th atom.<sup>d</sup>Structure also contains seven- and eight-coordinate (unknown geometry) Th atom.

d = distorted, poct = pseudo-octahedral, bctp = bicapped trigonal prismatic, sqap = square antiprismatic



**Figure Captions.**

**Fig. 1.** General view of the crystal structure of  $\text{Ba}_3\text{ThSe}_3(\text{Se}_2)_2$  projected along the  $b$ -axis.

**Fig. 2.** Local coordination environment of Th atoms in the  $\text{Ba}_3\text{ThSe}_3(\text{Se}_2)_2$  structure.

**Fig. 3.** Local coordination environment of Ba1 and Ba2 atoms in the  $\text{Ba}_3\text{ThSe}_3(\text{Se}_2)_2$  structure.

**Fig. 4.** Comparison of (a) the  ${}^2_{\infty}[\text{AnS}_6^{4-}]$  layers in the  $\text{Ba}_2\text{AnS}_6$  (An = Th, U) [19] structure with (b) the  ${}^1_{\infty}[\text{ThSe}_7^{6-}]$  chains in the  $\text{Ba}_3\text{ThSe}_3(\text{Se}_2)_2$  structure.

**Fig. 5.** Optical absorption spectrum of  $\text{Ba}_3\text{ThSe}_3(\text{Se}_2)_2$ .

**Fig. 6.** Analysis of  $\alpha^2$  and  $\alpha^{1/2}$  vs. energy for  $\text{Ba}_3\text{ThSe}_3(\text{Se}_2)_2$ .

**Fig. 7.** Total and partial density of states (DOS) of  $\text{Ba}_3\text{ThSe}_3(\text{Se}_2)_2$ .

Figure 1

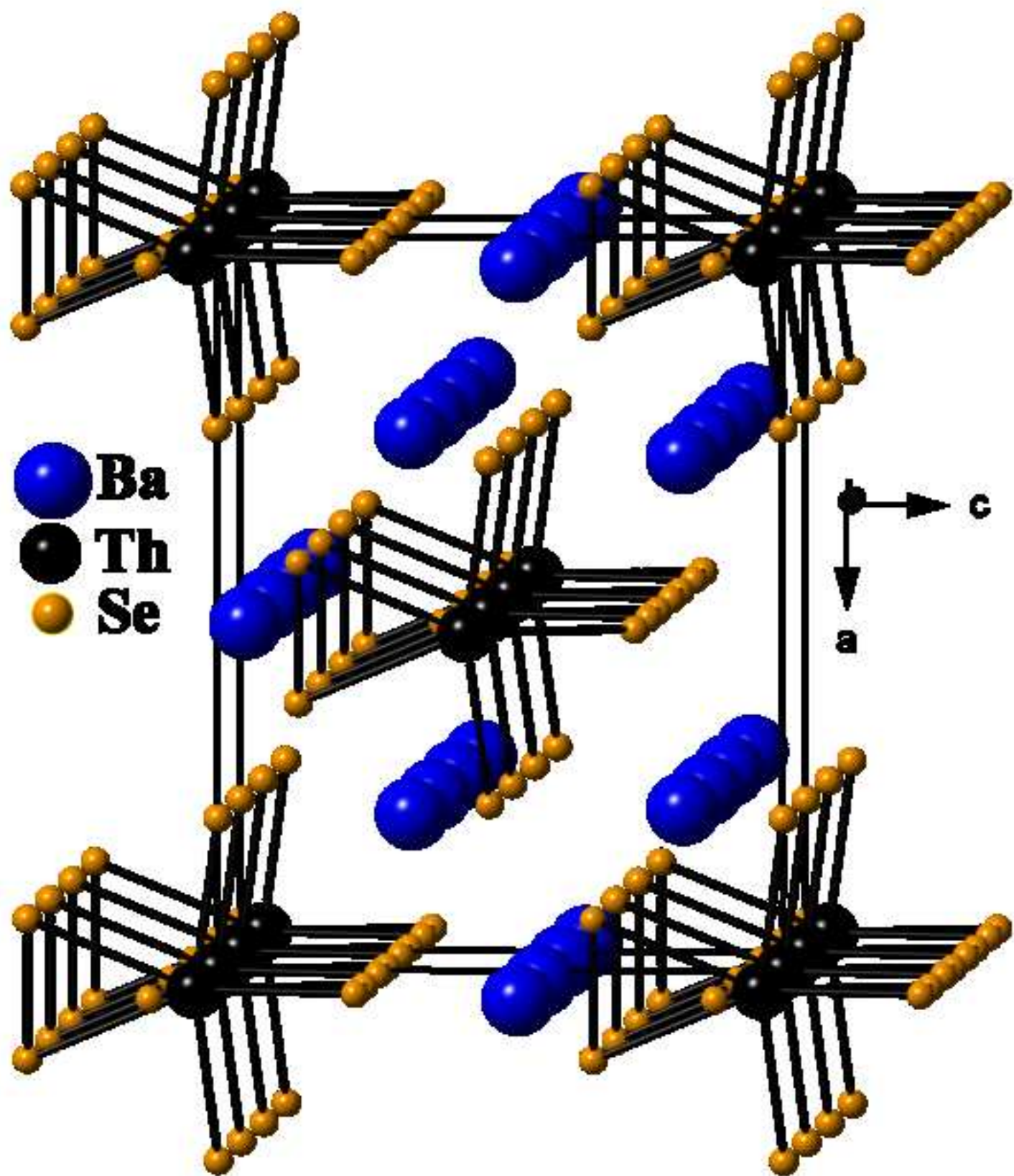


Figure 2

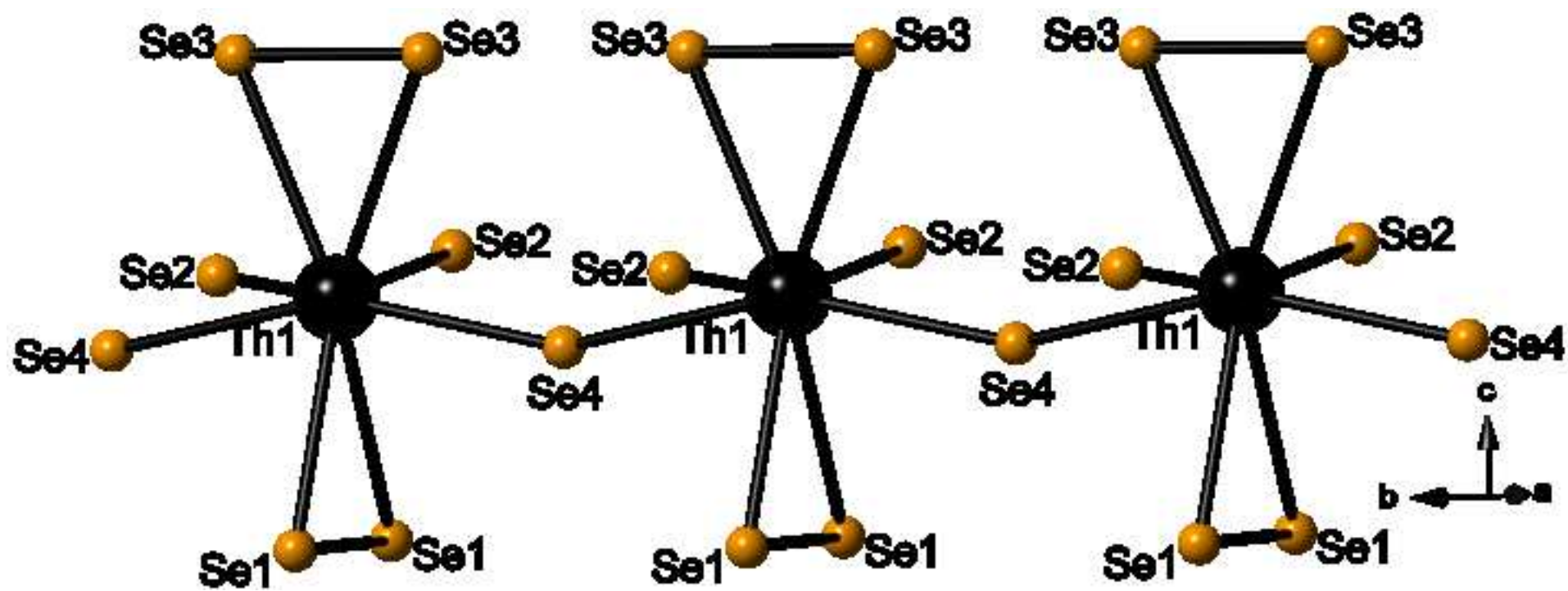


Figure 3

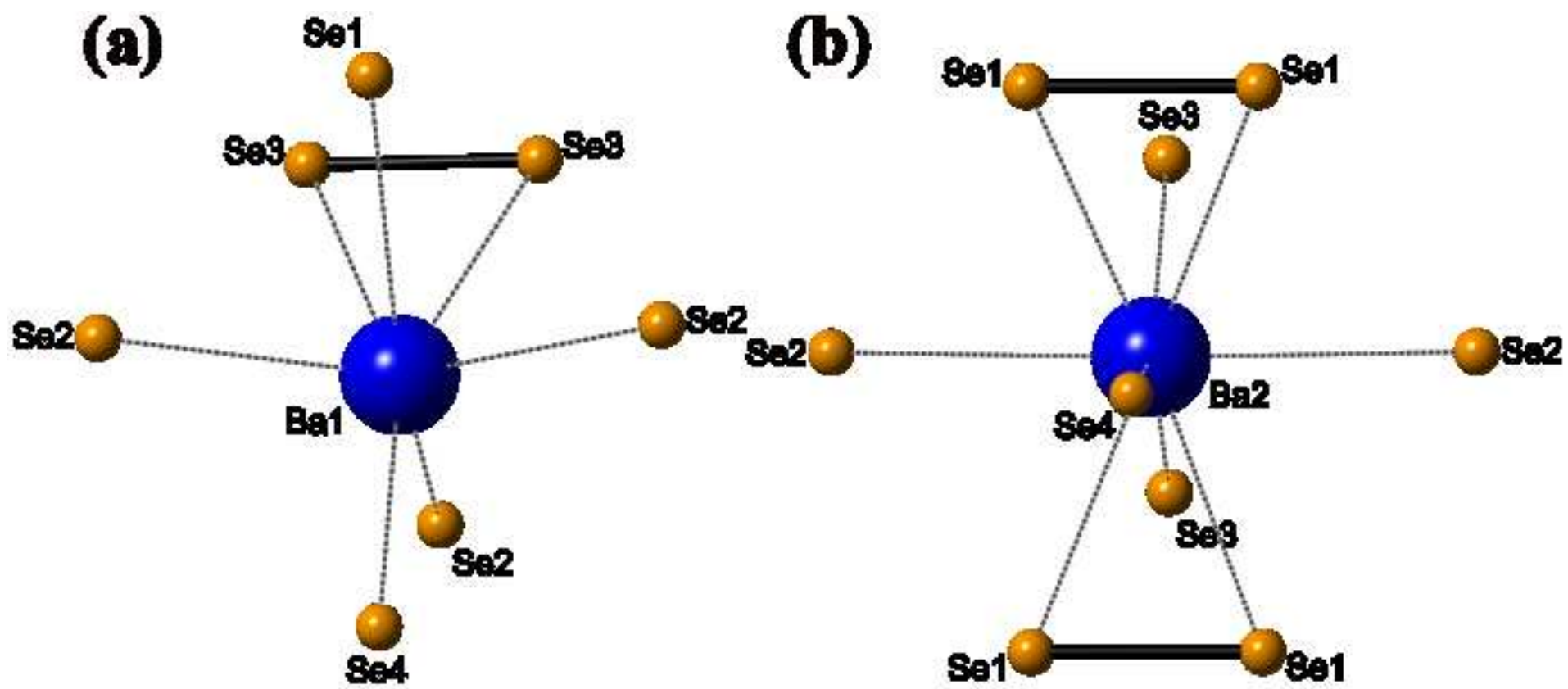


Figure 4

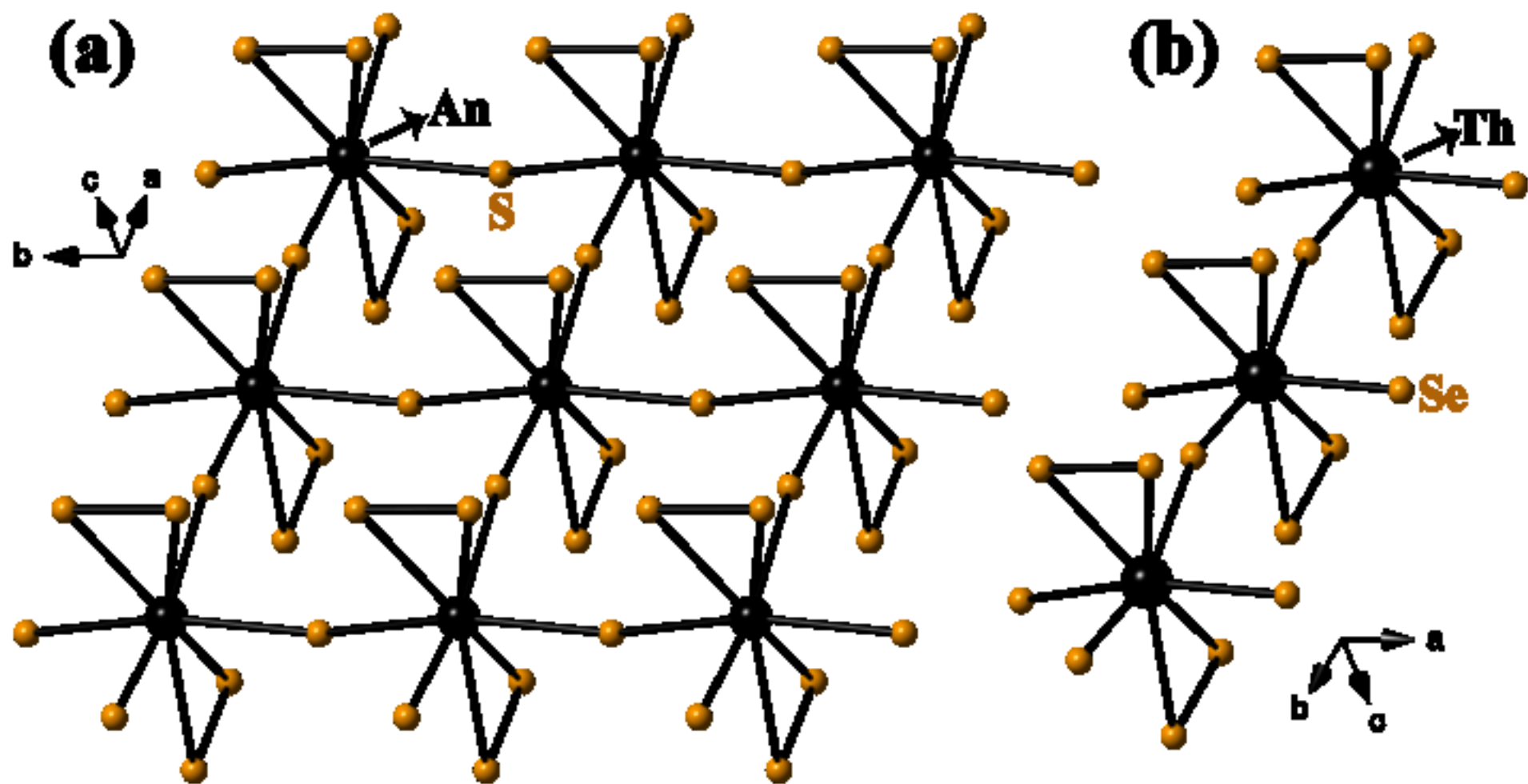


Figure 5

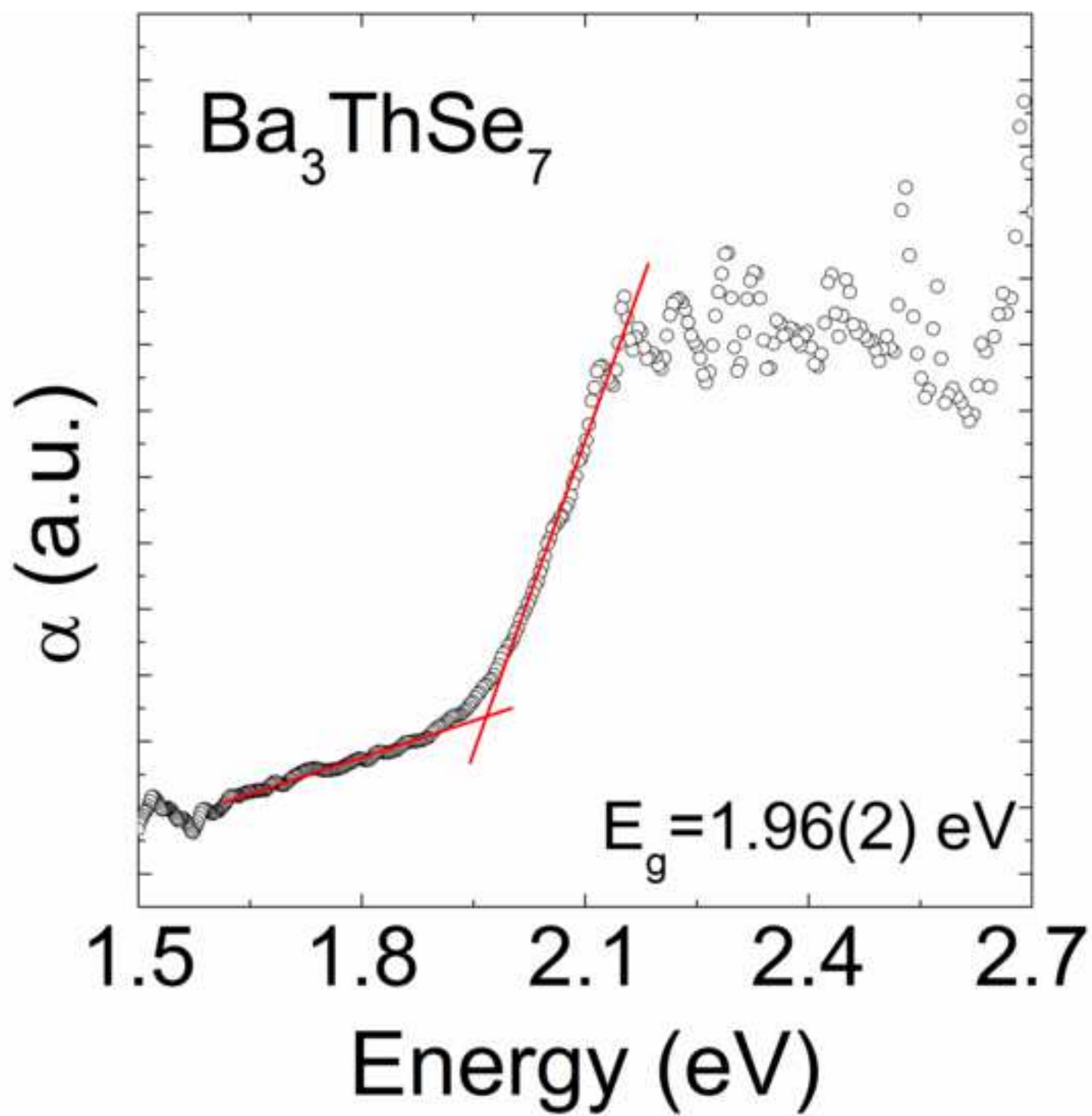


Figure 6

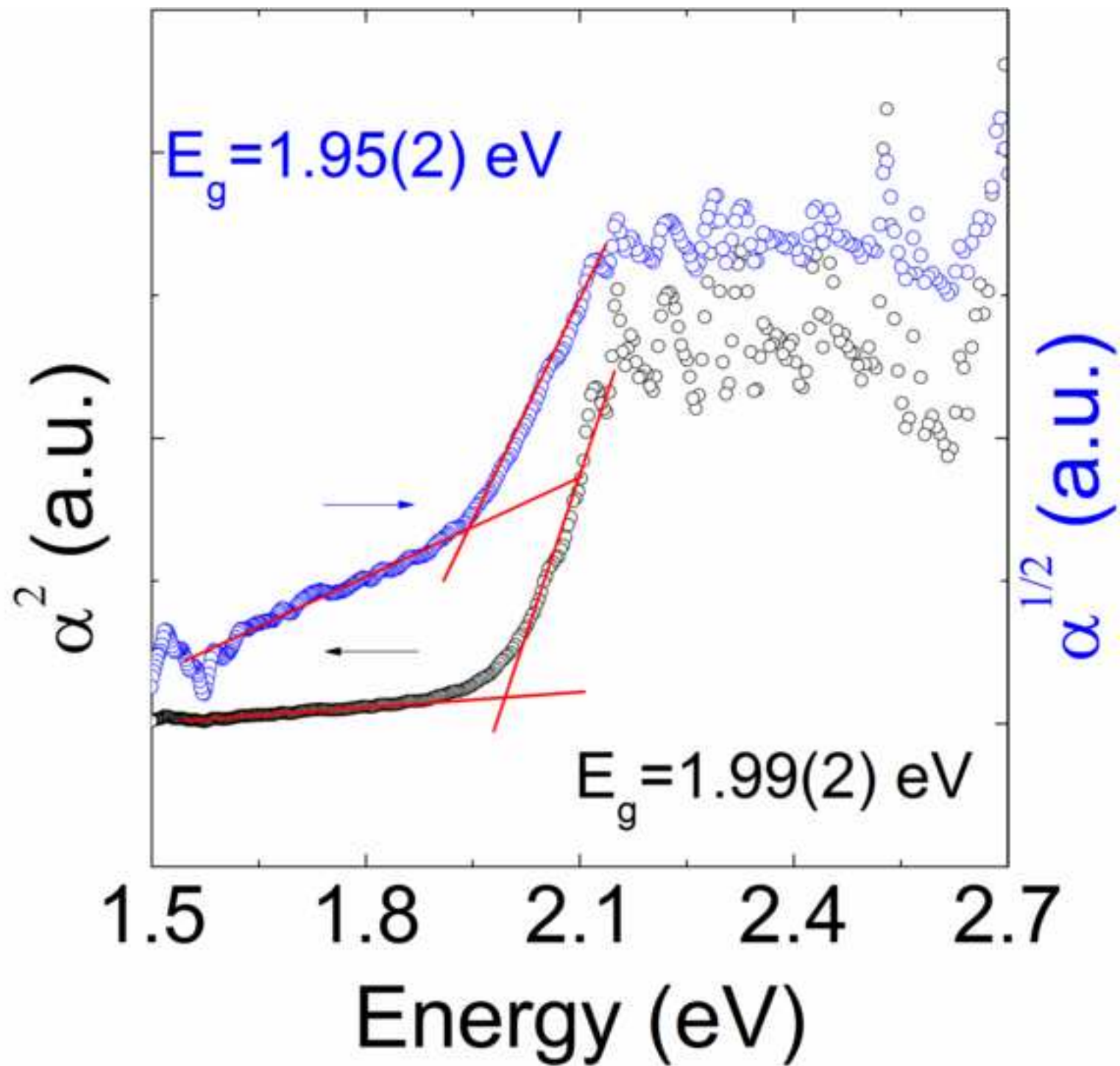
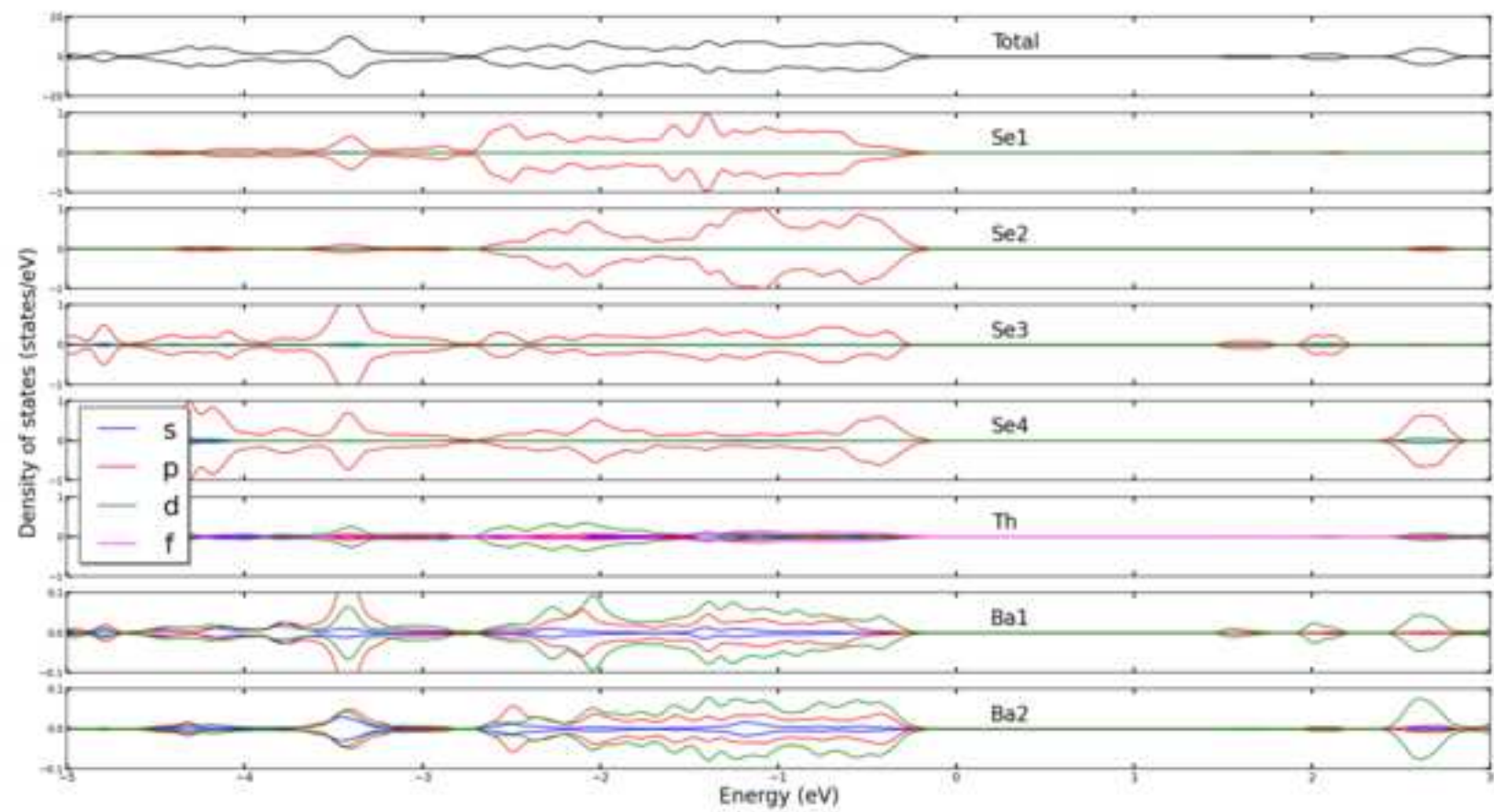


Figure 7



Local coordination environment of Th atoms in the  $\text{Ba}_3\text{ThSe}_3(\text{Se}_2)_2$  structure

